Frequency Agile 2×2 Micromachined Antenna Array

Ashish Kumar Chauhan, Ayan Karmakar and Kamaljeet Singh

Abstract – **The present work summarizes the design and development of 2×2 micromachined patch antenna array. Wafer thinning is carried out to cater for high frequency operations. Detailed design methodology with fabrication process steps is outlined in this article. A new concept of composite (Silicon-Glass) substrate synthesizing along with micromachined structure has been presented to shift the operating frequency band of the antenna. Comparative study is carried out for various antenna configurations. A good agreement is observed between the experimental results and simulated values.**

Keywords – **Micromachined antenna, microstrip, High resistivity silicon (HRS), frequency agility.**

I. INTRODUCTION

Microstrip patch antennas are gaining popularity in space, defence, air-borne and mobile communication systems due to its compact size, light weight and miniaturized features. Bulky antenna elements using 3-D structure are replaced with compact planar topology [1-3]. But, this low profile antenna mainly suffers for its inherent low bandwidth and gain characteristics. Micro electromechanical systems (MEMS) can be used effectively to eradicate these short comings [4-7]. Implementing the bulk micromachining in antenna designing makes the patch antenna highly efficient. Thicker substrate with low permittivity can be synthesized using MEMS, which in turn help to attain desired antenna performances [8-10]. Antennas with frequency agility and polarization diversity can also be realized with MEMS [11-14]. Furthermore utilizing CMOS process, tight fabrication tolerances can be obtained at higher operating frequencies. Silicon being a prime choice for micromachining also helps to realize antenna with integrated electronics, desired for SoC concept.

The present work demonstrates the development of a prototype micromachined 2×2 antenna array on high resistivity silicon HRS (ρ > 8kΩ-cm, tan δ = 0.01) substrate. Detailed design with process steps has been outlined in this article. Process variation is taken into account to predict alteration in overall performance of the antenna. Frequency agility of the antenna structure has been achieved by embedding composite dielectrics beneath the radiating elements. Measured results show a very close agreement with predicted simulated values.

II. ANTENNA DESIGN

This section covers in detail the design of micromachined antenna with three sub-sections: Conventional micromachined antenna design, effect of membrane thickness and composite (Si-Glass) substrate effect.

Ashish Kumar Chauhan, Ayan Karmakar and Kamaljeet Singh are working in Semi-Conductor Laboratory, Punjab, India, E-mail: ayanns@gmail.com

Targeted specification is depicted in Table 1.

TABLE 1
TARGETED SPECIFICATION OF ANTENNA ARRAY

Parameter	Values
Centre Frequency(GHz)	14.5
Fractional bandwidth (%)	3-5
Return Loss @f_0 (dB)	>15
Gain(dBi)	> 10
E and H-plane beam-width (degree)	~ 70
Side lobe Level (dBc)	> 20
Polarization	Linear
Radiation Efficiency (%)	> 90

A. Conventional Micromachined Antenna Design

It starts with the design of corporate feed network, depicted in Fig. 1. All dimensions are in micron in this figure. Standard 50 Ω input line is bifurcated into two quarter-wave long 70.7 Ω transmission lines, which again terminated with 50 Ω lines. The same technique is repeated twice to feed four radiating patches. The distance between two adjacent patch elements is kept as 0.75 λ_0 and the whole structure looks symmetrical with respect to the axis passing through its input feed line. This feed network is little different than its conventional counterparts. Optimal radiation characteristic has been obtained to have a deep null at the boresight direction, for special application of this antenna.

The distance between two maximally spaced elements is 27.2 mm, which is nearly equivalent to 1.25 λ_0, which gives a difference in phase shift of 90°. An array of 2×2 size is targeted here, which can be repeated to get much higher directive gain of the whole assembly.

Further, micromachining of silicon beneath the patch make the structure more radiation efficient. Optimum value of the silicon membrane thickness is ~50 μm, considering fabrication constraints and overall antenna performances. Dimension of the micromachined antenna element can be obtained by the following governing equations [4].

$$\varepsilon_{reff} = \varepsilon_{cavity}\left(\frac{L + 2\Delta L\frac{\varepsilon_{fringe}}{\varepsilon_{cavity}}}{L + 2\Delta L}\right) \quad (1)$$

$$\frac{\varepsilon_{fringe}}{\varepsilon_{cavity}} = \frac{\varepsilon_{air} + (\varepsilon_{sub} - \varepsilon_{air})x_{air}}{\varepsilon_{air} + (\varepsilon_{sub} - \varepsilon_{air})x_{fringe}} \quad (2)$$

$$\varepsilon_{cavity} = \frac{\varepsilon_{air}\varepsilon_{sub}}{\varepsilon_{air} + (\varepsilon_{sub} - \varepsilon_{air})x_{air}} \quad (3)$$

where,
L = length of the micro-machined patch
ΔL = infinitesimal increment in patch length due to fringing effect
ε_{reff} = effective dielectric constant of the micromachined substrate (air & silicon)
ε_{air} = permittivity of air
ε_{sub} = permittivity of the dielectric substrate
x_{air} = ratio of the air to full substrate thickness in the mixed field region
x_{fringe} = ratio of the air to full substrate thickness in the fringing field region (=0, in this case)

The effect of micromachining on antenna performances is highlighted in Table 2. It shows considerable performance improvement compared to conventional topologies.

TABLE 2
EFFECT OF MICROMACHINING ON CONVENTIONAL PATCH ANTENNA

Parameter	Conventional Patch	Micromachined Patch
Return Loss (dB)	21.5	32.1
Fractional Bandwidth (%)	3.3	9.03
Peak Gain (dB)	2.39	5.31
Peak Directivity (dB)	2.82	5.47
Radiation Efficiency (%)	90.64	96.41

B. Effect of Membrane Thickness

Bulk-micromachining of the silicon substrate beneath the patches results in thin membrane. The thickness of the membrane basically dictates the resonant frequency of the antenna. FEM based analysis is performed to find out the role of membrane thickness on the return loss parameter, shown in Fig.2. Cavity of the antenna is opened at the back side of the wafer using bulk removal of Si in KOH solution. Standard 40 % KOH solution at 80˚C is used for this purpose, which gives an approximate etch rate of silicon as1.1 to 1.3 µm/min.

During this anisotropic etching of silicon, variation in the membrane thickness can be found for different cavities in the array antenna. This practical phenomenon has been studied on single antenna element, summarized in Table 3. From the analysis, it can be inferred that as the membrane thickness increases, the resonant frequency shifts towards lower value, without affecting all other antenna parameters. It is because of change in effective permittivity seen by the radiating elements. As the thickness of the membrane increases, the effective dielectric constant of the composite substrate (silicon & air) approaches towards higher permittivity. With the enhancement of effective permittivity, the guided wavelength also increases, which in turn lowers the resonant frequency. Effective permittivity is altered due to varied membrane thickness as per Eqn. (1)-(3).

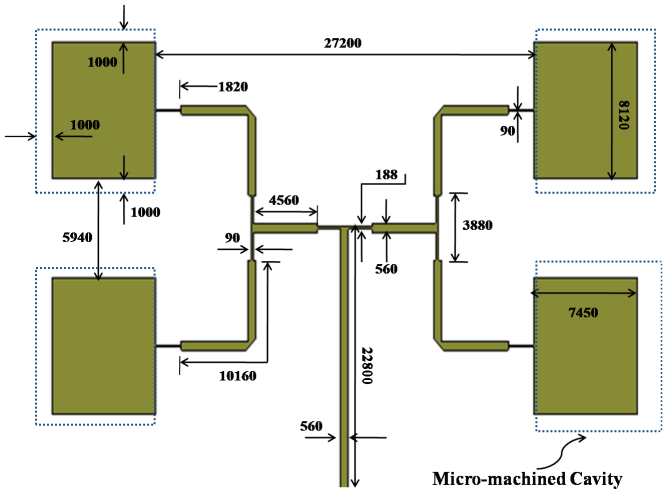

Fig. 1. Top-view of patch antenna array with feed network (all dimensions are in micron)

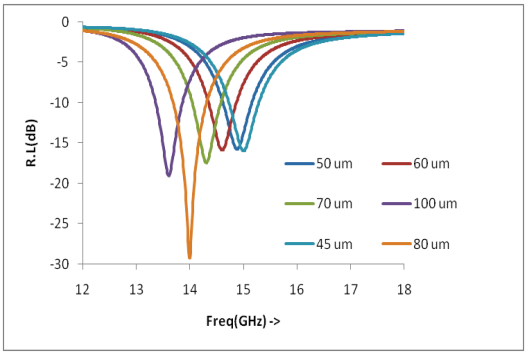

Fig. 2. Return loss variation of antenna with membrane thickness

TABLE 3
VARIATION OF ANTENNA PARAMETERS WITH MEMBRANE THICKNESS

t (µm)	f_0 (GHz)	R.L @f_0 (dB)	FBW (%)	G_P (dB)
45	15.00	-15.95	3.67	4.87
50	14.80	-15.90	3.73	3.85
60	14.61	-15.83	3.53	5.75
70	14.31	-17.40	3.71	5.60
80	14.00	-29.20	7.46	5.46
100	13.60	-19.00	3.67	4.87

t = membrane thickness, f_0 = resonant frequency, R.L = return loss, FBW = fractional bandwidth & G_P = peak gain

C. Composite Substrate Effect

This subsection mainly focuses on the effect of composite substrate on the antenna performance. It has been observed that, the resonant frequency of the array structure can be shifted upward or downward in the frequency spectrum by

sandwiching commonly available microwave substrates. In this way, the operating band can be agile without modifying the actual patch dimensions. In the proposed antenna configuration, without altering physical dimensions of the array structure, effective dielectric constant of the substrate can be changed by stacking up various substrates beneath silicon. The equivalent lumped model of the transmission line in that situation can be modeled as shown in Fig. 3.

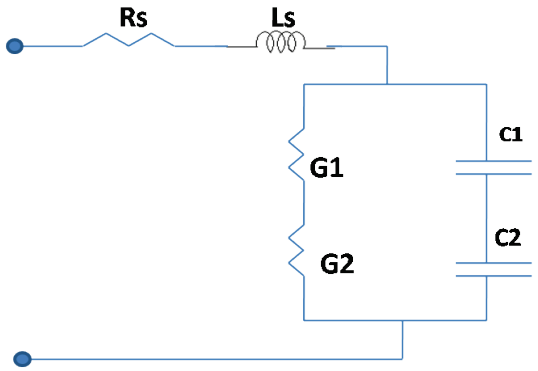

Fig. 3. Lumped equivalent circuit of the transmission line on stacked substrate configuration

In this CLR-model, the G1, G2, C1 and C2 terms come due to various substrate effects. G1 and C1 are due to the silicon and the G2 and C2 are for glass material. The effective conductance and the capacitance of the transmission line alter this way. For the high frequency circuit application, in most of the cases the effect capacitance value dominates the G-value. Minimum the value of the C(either C1 or C2) basically dictates the equivalent capacitance of entire circuit topology. And, this C-value is a function of the thickness and the dielectric constant of the sandwiched substrate.

And, in the rectangular patch antenna configuration as chosen in this work TM_{10} mode is the lowest order mode and possesses the lowest resonant frequency of all the time harmonics modes. The narrowband model for this TM_{10} mode can be expressed as shown in Fig. 4 [10].

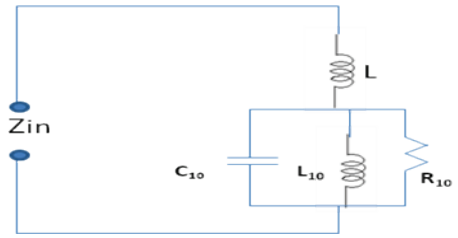

Fig. 4. Narrowband model for the TM_{10} mode

In this circuit, the value of the capacitance (C_{10}) changes due to the stacked substrate configuration, which further alters the resonance frequency of the antenna. In this way, the operating frequency of the patch antenna shifts from one microwave band to other.

A generic pictorial representation of the antenna with composite substrate is shown in Fig. 5.

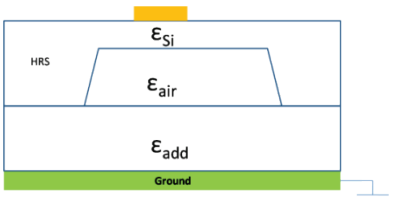

Fig. 5. Generic cross-sectional view of micromachined antenna with added substrate

In this configuration, the equivalent permittivity can be obtained as,

$$\frac{1}{\varepsilon_{eq}} = \frac{1}{\varepsilon_{si}} + \frac{1}{\varepsilon_{air}} + \frac{1}{\varepsilon_{add}} \quad (4)$$

or, $\frac{1}{\varepsilon_{eq}} = \frac{1}{\varepsilon_{const.}} + \frac{1}{\varepsilon_{add}}$ [As, in this case the the geometry of the micro-machined antenna is kept constant.]

$$\textbf{Now,} \quad \varepsilon_{add} \propto \frac{\varepsilon_r}{d_r} \quad (5)$$

where,

ε_{eq} = equivalent permittivity of the stacked substrate (silicon, air and added substrate)

ε_{air} = permittivity of air

ε_{si} = permittivity of the dielectric substrate

ε_{add} = permittivity of added substrate

In the present scenario, the cavity depth and the thickness of the bulk silicon remains constant (resulting in $\varepsilon_{const.}$), only the type of sandwiched material is changed. Such four different cases have been studied using available resources to us. Fig. 6 explains the cases by depicting the cross-sectional views of the basic structure. Table 4 summarizes the effect of composite substrate on the antenna performance. Now, for a particular sandwiched substrate (ε_r), as its thickness (d_r) increases, ε_{add} decreases, which further results in decrement of equivalent permittivity of the composite substrate and resonant frequency (f_0). This effect has been shown in Table-4 (case II & IV), where the same dielectric material (glass) is used with different thicknesses (0.5 mm and 1 mm). It can be inferred that, a shift from K_u to X-band is achieved with only embedding an extra dielectric material between the antenna structure and ground plane. Fractional bandwidth and radiation efficiency is enhanced drastically in Case-II. So, we fabricate this configuration to characterize the antenna structure.

TABLE 4

COMPOSITE SUBSTRATE EFFECT ON ANTENNA PERFORMANCE

Structure	f_0 (GHz)	R.L @f_0 (dB)	FBW (%)	G_P (dB)
Silicon μ-machined	14.61	-15.83	3.53	5.75
I	10.22	-17.96	6.16	2.90
II	10.83	-21.5	11.6	3.17
III	11.84	-36.7	5.37	4.68
IV	11.82	-14.4	5.14	4.18

f_0 = resonant frequency, R.L = return loss, FBW = fractional bandwidth & G_P = peak gain (structures I, II, III & IV correspond to Fig. 6)

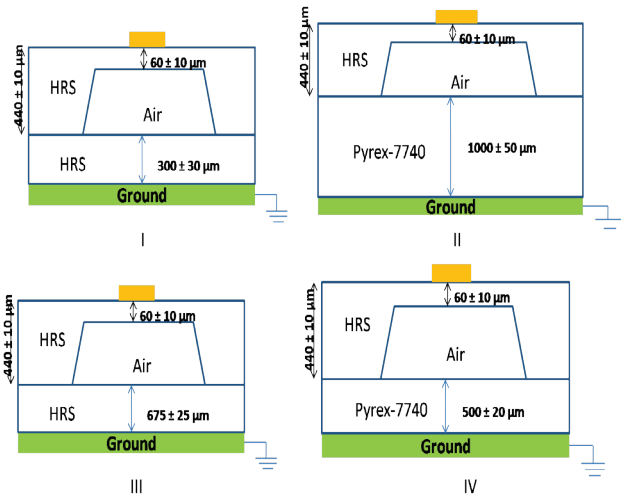

Fig. 6. Cross-sectional view of various micromachined antenna configurations with Composite Substrates

III. Fabrication and Measured Results

Fabrication of the antenna structure starts with standard 6" high resistive silicon wafer of 675±20 µm thickness and resistivity of the order of 8kΩ-cm. After giving the conventional chemical cleaning treatment, 500Å base oxide is grown on the wafer, which acts as buffer layer for the subsequent RF circuits printed on this. 1 µm thick aluminum is sputtered and patterned subsequently on the front side of the wafer to realize metallic antenna patches with feed network. A thick passivation/protective layer is coated thereafter on the front side, which is followed by thinning of wafer up to 440 µm with KOH solution. This thin wafer is patterned and etched in KOH solution from the backside to form cavities with 50 ±10 µm membrane thickness underneath patches. Finally the front side passivation layer is removed in suitable solution. Fig. 7 depicts the top and bottom views of fabricated micromachined prototype antenna array.

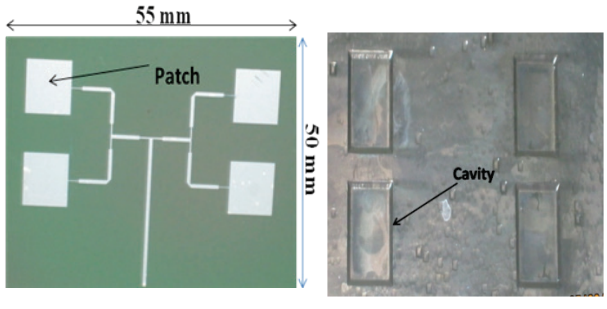

(a) (b)

Fig. 7. (a) Top view and (b) bottom view of the micromachined antenna array

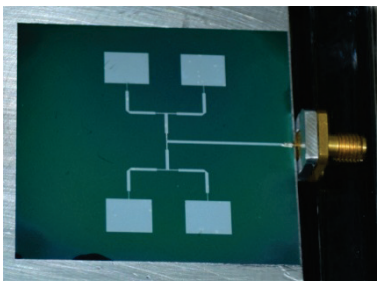

Fig. 8. Test fixture with antenna array mounted

For characterizing the circuit, the fabricated structure is diced with standard dicing tool and then it is assembled on aluminum jig (working as microstrip ground plane) with RF connector (2.92 mm), shown in Figs. 8 and 9, respectively. With the present in-house facility, only the return loss characteristic has been measured using R&S make Vector Network Analyzer ZVA-40. And, the far-field radiation pattern measurement for the compact range is underway. Simulated 3D radiation pattern is shown in Fig.10. It shows that, there is dip in the gain value at the boresight direction. Peak gain of the antenna array is coming around 12.8 dBi.

This kind of antenna can find wide applications in wireless and RADAR. Specially, in radar communication, while a jamming signal is essential, difference pattern of the antenna is generated. The difference pattern consists of a null in the boresignt direction with two major lobes adjacent to null. The null in the difference pattern suppress the source of the jamming signal and finally the tracking accuracy is improved [15 & 16].

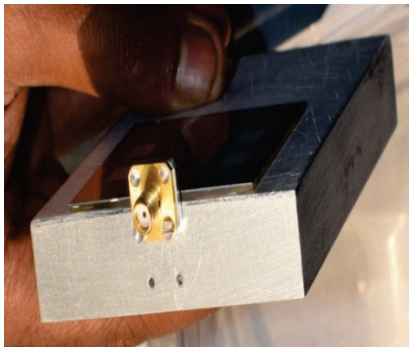

Fig. 9. Micromachined antenna structure on composite substrate (Case-II of Table-4)

Measured S-parameter results show a very close coherence with the predicted simulated values, as shown in Figs. 11 and 12 and summarized in Table 5. It has been observed that, a simple micromachined antenna array operating in Ku-band (14.9 GHz) with 4.4 % fractional bandwidth can be switched to X-band (11.1 GHz) with a drastic improvement in fractional bandwidth as 7.6 % by implementing the proposed composite substrate configuration. This observation is attributed to the fact that, micromachining results in reduction in surface wave losses, thereby increasing overall space wave losses (i.e. radiation) from the antenna. So this increased radiated energy decreases the quality factor (Q), which tends to enhance the antenna bandwidth (BW), as BW varies inversely with Q [1, 8 & 9].

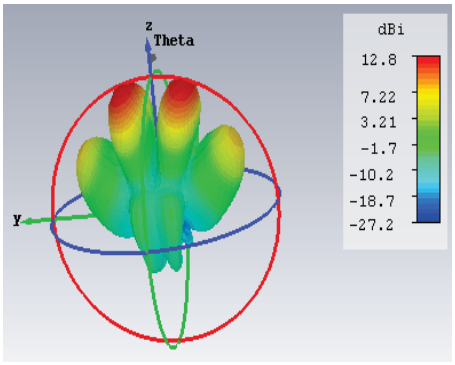

Fig. 10. Simulated 3D radiation pattern of the antenna array

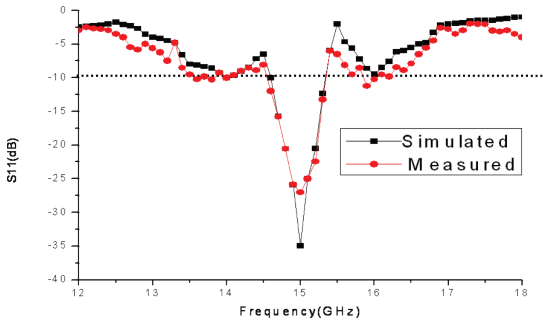

Fig. 11. Measured and simulated results for the silicon micromachined antenna array

TABLE 5
MEASURED RESULTS COMPARISON OF MICROMACHINED ANTENNA ARRAY WITH AND WITHOUT GLASS SUBSTRATE

Parameter	Micromachined antenna array		Glass embedded micromachined antenna array	
	Spec.	Meas.	Spec.	Meas.
Resonant Frequency (GHz)	14.6 ± 0.3	14.9	10.8 ± 0.3	11.1
R.L (dB) @ f_0	> 12	27	> 12	14
FBW (%)	> 3	4.41	> 3	7.61

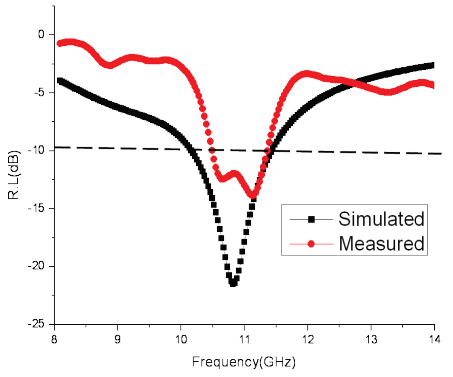

Fig.12. Measured and simulated results for the silicon micromachined antenna array with stacked glass substrate

IV. CONCLUSION

A simple micromachined antenna array is presented in this work. Detailed design methodology with fabrication process is discussed. Patch antenna with 7.6 % bandwidth and better than 12 dB return loss is realized. A new technique for frequency agility is adopted. Without altering the actual patch or feed network's geometry, the operating frequency of the proposed array can be tuned from K_u-band to X-band easily, using the composite substrate concept. Light weight, compact profile and frequency alteration capability make the present design an attractive choice for space, defence and any other civilian applications. Specially, in RADAR communication this kind of frequency agile antenna is demanded. Null at the boresignt direction makes this antenna suitable for radar jamming purpose.

ACKNOWLEDGEMENT

The authors are very much grateful to Sh. Surinder Singh (Director-SCL) for his continuous support and motivation during this work.

REFERENCES

[1] D. M. Pozar, *Microwave Engineering*, John Wiley and Sons Inc., New York,1998.
[2] D. M. Pozar, D. H. Schaubert, *Microstrip Antennas – The Analysis & Design of Microstrip Antennas & Arrays*, John Wiley & Sons, Inc., Hoboken, New Jersey, 1995.
[3] K. R. Carver, J. Mink, "Microstrip Antenna Technology", *IEEE Trans. on Antennas & Prop.*, vol. 29, no. 1, pp. 2-24, 1981.
[4] I. Papapolymerou, R. F. Drayton, L. P.B. Katehi, "Micromachined Patch Antennas", *IEEE Transactions on Antennas and Propagations*, vol. 46, no. 2, pp. 275-283, February 1998.
[5] G. P. Gauthier, A. Courtay, G. M. Rebeiz, "Microstrip Antennas on Synthesized Low Dielectric-constant Substrates", *IEEE Transactions on Antennas and Propagation*, vol. 45, pp. 1310-1314, Aug. 1997.
[6] S. Lucyszyn, S. Pranonsatit, "RF-MEMS for Antenna Applications," *Proceeding of 7th European Conference on Antennas and propagation (EUCAP)*, pp. 1988-1992, 2013.
[7] L. P.B. Katehi, "Si Micromachining for High Frequency Appications," *Yugoslav IEEE MTT Chapter Informer*, vol. 4, *December 1996.*
[8] R. Garg, P. Bhartia, I. Bahl, A. Ittipiboon, *Microstrip Antenna Design Handbook*, Artech House, 2001.
[9] C. A. Balanis, *Antenna Theory: Analysis and Design*, John Wiley and Sons Inc, New York, 1997.
[10] R. Bancroft, *Microstrip & Printed Antenna Design*, SciTech Publisher Inc., 2004.
[11] E. Chang, S. A. Long, W. F. Richards, "An Experimental Investigation of Electrically Thick Rectangular Microstrip Antennas", *IEEE Transactions on Antenna and Propagation*, vol. AP-34, no. 6, pp. 767-772, June 1986.
[12] R. N. Simons, D. Chun, L. P.B. Katehi, "Reconfigurable Array Antenna Using Microelectromechanical Systems (MEMS) Actuators," *NASA GRC Report,* no. NASA/CR-2001-210889, April 2001.
[13] R. N. Simons, D. Chun, L. P.B. Katehi, "Polarization Reconfigurable Patch Antenna Using Microelectromechanical

Systems (MEMS) Actuators", *NASA GRC Report*, no. NASA/TM-2002-211353, April 2002.

[14] A. Karmakar, A. Kaur, K. Singh, "Ku-band Reconfigurable MEMs Antenna on Silicon Substrate", *9th International RADAR Symposium India (IRSI-13)*, 2013.

[15] T.A. N.S.N Varma, G. S.N. Raju, "Investigations on Generations of Very Low Sidelobe Difference Patterns for EMC Applications", *IOSR-Journal of Electronics and Communication Engineering*, vol. 9, no. 3, Ver. VI (May-June, 2014), pp. 8-13.

[16] Rohde & Schwarz's White paper on "Introduction to Radar System and Component Tests," *No.08_2012_1MA207_0e*.